Available online at www.worldscientificnews.com

World Scientific News

An International Scientific Journal

WSN 149 (2020) 36-51 EISSN 2392-2192

Modified Integrated Nuclear Model for the Binding Energy of Finite Nuclei

Hezekiah K. Cherop and **Kapil M. Khanna***

Department of Physics, University of Eldoret, P.O Box 1125-30100, Eldoret, Kenya

*E-mail address: khannak700@gmail.com

ABSTRACT

A modified integrated nuclear model (MINM) for calculating the binding energies of finite nuclei is proposed. The model is an improvement of the integrated nuclear model (INM) that was formulated based on the theory of quantum chromodynamics. MINM is a simple model that depends on the proton and neutron numbers, and a variable stability coefficient factor denoted by λ. The variable λ rectifies the inequality in the neutron to proton ratio that results from the increase in the size of the nucleus. The results of the binding fraction obtained from MINM were compared with the existing experimental data obtained from atomic mass evaluation tables, AME2016. It was found that, the root mean square deviation for the binding fractions obtained from MINM is 0.2267 MeV with respect to the experimental data, while the root mean square deviation for the binding fraction obtained from INM is 1.5801 MeV. The root mean square deviation for MINM is very small. This supports the validity of the MINM and the consequent accuracy in the values of the binding fraction for different nuclei, especially in the region whereby A>220.

Key words: Nuclear model, binding energy, binding fraction, nuclei

1. INTRODUCTION

It is now well known that, the nucleus of an atom is a highly complex quantum system composed of protons and neutrons [1]. Besides, a very strong short-range force holds the

(Received 19 August 2020; Accepted 05 September 2020; Date of Publication 06 September 2020)

protons and neutrons together while the electrons orbit the nucleus in specified orbits having certain energy levels [2]. However, the exact nature of interaction of particles inside the nucleus remains to be unknown [3]. Several scientific efforts both experimental and theoretical are in place to unravel the mysteries in the nucleus of an atom [4]. These attempts include formulation of nuclear models and developing powerful accelerators for investigating nuclear reactions (using radioactive ion beams) that are crucial in synthesizing new elements and isotopes [5].

During the formation of a nucleus of mass number A from Z protons and N neutrons, which are completely separated from each other [2, 6], a small amount of mass of the constituent nucleons is converted into energy [7]. This energy is called the binding energy and it forms the basis of understanding the properties of atomic nucleus [8].

The binding energy of the nuclei is of essence in describing the properties of the finite nuclei. Firstly, it gives information on stability of all the nuclei since the nuclei that have different number of protons and neutrons have different binding energies resulting into different decay probabilities [9]. Secondly, the binding energy may act as a tool that can predict the abundance of heavy elements that are rare on earth but present in neutron stars and other celestial bodies. This is due to the fact that, as the proton number increases, new shells get filled up creating fission barriers and thus the binding energy in the ground state increases resulting to greater stability for the nuclei. Consequently, the most stable nuclei become highly bound and chemically abundant.

Lastly, the binding energy determines the synthesis of the super heavy elements through nuclear fission or fusion process of the nuclei [10]. For the heavy nuclei ($A \geq 120$), the binding energy is significant in the process of cold fusion and hot fusion. In cold fusion, heavy targets such as lead or bismuth are bombarded with heavy ions of iron or nickel at energies above Coulomb barrier to form super heavy elements, while in hot fusion, the actinide targets are bombarded with calcium beams to form highly excited compound nucleus [11]. Currently, the hot fusion is the most successful technique in artificial synthesis of the super heavy nuclei.

2. THEORETICAL MODELS

Several mathematical models have been developed in the past to calculate the binding energies of nuclei. However, no single model has been able to generate exactly the experimental binding energy data especially among the super heavy nuclei. This is because the calculations of the binding energies are based on the rough estimates of the large number of nucleons (protons and neutrons) that are in collective motion. These mathematical models include:

(i) Bethe-Weizsäcker semi-empirical mass formula (B-WSEMF)

This model was formulated by a German Physicist, C.F Von Weizsäcker in 1935 [12]. The insights behind the formulation of this famous model emanated from the concepts of the liquid drop model (LDM), that was first proposed by a Russian Physicist G. Gamow in 1928 [13] and later improved by N. Bohr and J. Wheeler [14].
The B-WSEMF is written as [12, 15-17];

$$B(A,Z) = a_1 A - a_2 A^{\frac{2}{3}} - a_3 \frac{Z(Z-1)}{A^{\frac{1}{3}}} - a_4 \frac{(A-2Z)^2}{A} \pm \delta(A) \quad (1)$$

where A is the mass number, Z is the atomic number, $a_1 = 15.99MeV$ represents the coefficient that is related to the volume term, $a_2 = 18.34MeV$ represents the coefficient of the surface term, $a_3 = 0.71MeV$ represents the coefficient that is associated with the Coulomb term, $a_4 = 23.21MeV$ represents the coefficient of the asymmetry term and $\pm\delta(A)$ is the pairing energy correction term.

B-WSEMF is credited for being the first phenomenological semi-empirical mass formula, that explains some crucial nuclear properties such as the mass parabola, binding fractions, fusion, fission and alpha-decay barrier potential [8, 18, 19]. However, B-WSEMF is limited in describing other nuclear properties such as magic numbers, nuclear magnetic moments, nuclear excited states and binding energies of light nuclei that are away from the line of stability [20, 21]. In regard to this, several modifications of B-WSEMF have been undertaken with a view of formulating a model that mirrors the experimental data for both light and deformed super heavy nuclei [8, 22-26].

(ii) Global optimal mass formula (GOMF): The global approach of calculating nuclear masses entails developing an algorithm that reproduces all known nuclear masses accurately. This is achieved by adjusting the parameters in the algorithm to generate the known nuclear masses, and the nuclear masses that are away from the region of stability [27]. Kolesnikov [28] considered an inverse problem to develop the GOMF. According to GOMF, the binding energies of the nuclei that are far from the beta-stability line were described appropriately. In addition, GOMF considers the super heavy elements as part of a whole system thus it suffices the description of the energy of alpha-decay of super heavy nuclei.

(iii) The E-space Inter-Domain Interaction Potential (EIDIP) nuclear binding energy model: The EIDIP model was formulated by Michael Hwang through the application of E-space Inter-Domain Interaction nuclear charge radii model [29]. The EIDIP nuclear charge radii model consists of multi-nucleon nuclei and it is given by the sum of the nucleon core radius, strong interaction gap, nucleon shell radius and positron shell radius [29, 30]. EIDIP nuclear binding energy model differs from B-WSEMF in the manner in which they are formulated. B-WSEMF is developed from the assumptions of the liquid drop model while EIDIP nuclear binding energy model is built from the reference nuclear binding energy data [31]. The strengths of EIDIP model is that, it is a simple model that employs only basic calculus, and it yields data that are more accurate than the data produced by B-WSEMF.

(iv) Integrated Nuclear Model (INM): This model was developed by Nader Ghahramany and his group using the assumptions that nuclei are made of quark-gluon soup rather than nucleons [32-35]. INM is a very interesting formula for calculating nuclear binding energies close to the stability zone [36]. In comparison with other nuclear models for calculating binding energies, the INM is the simplest because it depends only on three basic nuclear parameters namely the atomic number (Z), neutron number (N) and mass number (A). Moreover, the calculations of binding fractions obtained from INM are relatively closer to the experimental data than other nuclear models for nuclei with $Z \leq 92$ [20].

On the contrary, accurate results are not obtained when INM is used to calculate the binding fraction of nuclei having $Z > 92$ (Transuranic elements and transactinides). The calculations of the binding fractions of such nuclei from the experimental data reveals that, the

binding fractions decrease progressively with increase in Z. However, calculations obtained from INM for $Z > 92$ tend to increase as Z increases. Till today, all the known nuclei with $Z > 92$, are artificial nuclei having very short half-lives, radioactive and deformed in their ground-state. Nonetheless, the "island of stability" has been predicted to accommodate some super heavy nuclei whose half-lives are in the order of millions of years [9]. Therefore, the gist of this research is to modify the integrated nuclear model in order to improve the accuracy of the binding fractions of all the finite nuclei.

3. MODIFIED INTEGRATED NUCLEAR MODEL

The binding energy equation for nuclei derived by Ghahramany and his group is written as [20, 34-35];

$$B(A,Z) = \left[3A - \left(\frac{\left(N^2 - Z^2\right) + \delta(N-Z)}{Z} \right) + 3^2 \right] * \frac{m_u c^2}{100} \text{ , for A > 5} \tag{2}$$

Ghahramany and his group developed the integrated nuclear model written in Eq. (2) from their physical intuition and the assumption that nuclei are made from quark-gluon soup instead of nucleons. This model yields good results of binding energies that are in agreement with available experimental data. Thus, it has been employed successfully to find the mass parabola and stability of isobaric nuclei [35]. However, the model requires minor corrections especially in the factor 3^2, to cater for the new experimental properties of nuclei that are discovered experimentally from time to time [8, 34].

Currently, one of the fundamental necessities in nuclear physics is to find out the nuclear masses and the binding energies of super heavy nuclei that are synthesized in heavy ion fusion and fission reactions [26]. As the nucleus increases in size beyond $Z > 92$, the neutron to proton ratio changes drastically contributing to the nucleon asymmetry term and Coulomb potential which is proportional to $\frac{(N-Z)^2}{3Z}$ [20,34]. In order to account for the binding energy resulting from the abnormal increase in the size of the nucleus, it is proposed that, the binding energy equation proposed by Ghahramany and his group can be modified such that the divisor in the second term can be replaced by $\sqrt{NZ}$. In addition, the factor 3^2 is replaced by a variable stability coefficient that is denoted by λ. This variable caters for the difference between the number of protons and neutrons. Based on these conditions, Eq. (2) can be written as:

$$B(A,Z) = \left[3A - \left(\frac{\left(N^2 - Z^2\right) + \delta(N-Z)}{\sqrt{NZ}} \right) + \lambda \right] * \frac{m_u c^2}{100} \quad \text{for A > 5} \tag{3}$$

where $m_u c^2 = 330$ MeV, the nuclear beta-stability line is defined as [20, 34-35];

$$\delta_0(\text{N-Z}) = \begin{cases} 0 \text{ for N} \neq \text{Z} \\ 1 \text{ for N} = \text{Z} \end{cases}$$

and the variable λ is defined as:

$$\lambda = \begin{cases} 9 \text{ for } Z \le 30 \\ 0.4Z \text{ for Z=31 to Z=59} \\ 0.5Z \text{ for Z=60 to Z=69} \\ 0.6Z \text{ for Z=70 to Z=79} \\ 0.7Z \text{ for Z=80 to Z=86} \\ 0.8Z \text{ for Z=87 to Z=92} \\ 0.9Z \text{ for Z=93 to Z=98} \\ Z \text{ for for Z=99 to Z=103} \\ 1.1Z \text{ for Z=104 to Z=110} \\ 1.2Z \text{ for Z=111 to Z=116} \\ 1.3Z \text{ for Z=117 and Z=118} \end{cases}$$

For nuclei with $Z \le 30$, the stability coefficient is constant, that is, $\lambda = 9$ as derived in integrated nuclear model. For $Z > 30$, the stability coefficient varies successively between $0.4Z$ to $1.3Z$, where Z is the atomic number. These parameters were chosen from our theoretical calculations as the best fits that give the values of the binding fractions that are very close to the experimental data.

4. RESULTS AND DISCUSSIONS

The calculations for the binding fractions using Eq. (3) are tabulated in Table 1.

Table 1. Nuclear binding energy per nucleon.

Nucleus	Z	A	B/A (MINM, MeV)	B/A (INM. MeV)	B/A (EXP, MeV)	Nucleus	Z	A	B/A (MINM, MeV)	B/A (INM. MeV)	B/A (EXP, MeV)
Li	3	6	4.767	4.767	5.332	Sc	21	45	8.828	8.769	8.619
	3	7	4.832	4.557	5.606	Ti	22	46	8.979	8.954	8.656
Be	4	9	5.940	5.775	6.463		22	47	8.872	8.818	8.661
B	5	10	6.864	6.864	6.475		22	48	8.774	8.681	8.723
	5	11	6.650	6.54	6.928		22	49	8.683	8.544	8.711
C	6	12	7.379	7.379	7.680		22	50	8.599	8.406	8.756
	6	13	7.144	7.065	7.470	V	23	50	8.817	8.732	8.696
	6	14	6.954	6.679	7.520		23	51	8.728	8.600	8.742

N	7	14	7.745	7.745	7.476	Cr	24	50	9.052	9.031	8.701
	7	15	7.508	7.449	7.699		24	52	8.857	8.779	8.776
O	8	16	8.018	8.018	7.976		24	53	8.771	8.652	8.760
	8	17	7.786	7.740	7.751		24	54	8.690	8.525	8.778
	8	18	7.590	7.425	7.767	Mn	25	55	8.810	8.700	8.765
F	9	19	8.007	7.970	7.779	Fe	26	54	9.114	9.096	8.736
Ne	10	20	8.399	8.399	8.032		26	56	8.930	8.862	8.790
	10	21	8.186	8.156	7.972		26	57	8.847	8.744	8.770
	10	22	8.000	7.89	8.080		26	58	8.769	8.626	8.792
Na	11	23	8.334	8.309	8.111	Co	27	59	8.881	8.785	8.742
Mg	12	24	8.651	8.651	7.901	Ni	28	58	9.168	9.152	8.732
	12	25	8.458	8.437	8.101		28	60	8.993	8.934	8.781
	12	26	8.286	8.208	8.334		28	61	8.913	8.824	8.765
Al	13	27	8.564	8.546	8.332		28	62	8.839	8.714	8.795
Si	14	28	8.831	8.831	8.448		28	64	8.703	8.493	8.777
	14	29	8.656	8.64	8.449	Cu	29	63	8.943	8.860	8.752
	14	30	8.498	8.439	8.521		29	65	8.801	8.647	8.757
P	15	31	8.736	8.722	8.481	Zn	30	64	9.048	8.996	8.736
S	16	32	8.965	8.965	8.493		30	66	8.900	8.790	8.760
	16	33	8.806	8.794	8.498		30	67	8.832	8.687	8.734
	16	34	8.660	8.614	8.583		30	68	8.768	8.583	8.756
	16	36	8.415	8.25	8.575		30	70	8.651	8.376	8.730
Cl	17	35	8.868	8.857	8.520	Ga	31	69	8.699	8.724	8.725
	17	37	8.602	8.515	8.570		31	71	8.581	8.524	8.718
Ar	18	36	9.070	9.070	8.520	Ge	32	70	8.776	8.857	8.722
	18	38	8.788	8.752	8.614		32	72	8.653	8.663	8.732
	18	40	8.558	8.424	8.595		32	73	8.597	8.565	8.705
K	19	39	8.973	8.965	8.557		32	74	8.543	8.467	8.725
	19	40	8.843	8.810	8.538		32	76	8.444	8.272	8.705
	19	41	8.726	8.655	8.576	As	33	75	8.612	8.604	8.701
Ca	20	40	9.153	9.153	8.551	Se	34	74	8.799	8.916	8.688

	20	42	8.893	8.863	8.617		34	76	8.681	8.733	8.711
	20	43	8.779	8.714	8.601		34	77	8.626	8.641	8.695
	20	44	8.675	8.565	8.658		34	78	8.575	8.549	8.718
	20	46	8.493	8.264	8.669		34	80	8.478	8.364	8.711
	20	48	8.338	7.961	8.667		34	82	8.390	8.179	8.693

Table 1. Continued

Nucleus	**Z**	**A**	**B/A (MINM, MeV)**	**B/A (INM. MeV)**	**B/A (EXP, MeV)**	**Nucleus**	**Z**	**A**	**B/A (MINM, MeV)**	**B/A (INM. MeV)**	**B/A (EXP, MeV)**
Br	35	79	8.640	8.675	8.688		48	106	8.733	8.932	8.539
	35	81	8.540	8.496	8.696		48	108	8.653	8.800	8.550
Kr	36	78	8.819	8.969	8.661		48	110	8.579	8.668	8.551
	36	80	8.706	8.795	8.693	Cd	48	111	8.543	8.601	8.537
	36	82	8.603	8.621	8.711		48	112	8.509	8.535	8.545
	36	83	8.555	8.534	8.696		48	113	8.476	8.468	8.527
	36	84	8.509	8.446	8.717		48	114	8.444	8.402	8.532
	36	86	8.423	8.271	8.712		48	116	8.383	8.269	8.512
Rb	37	85	8.569	8.57	8.697	In	49	113	8.554	8.627	8.523
	37	87	8.481	8.399	8.711		49	115	8.488	8.497	8.517
Sr	38	84	8.729	8.852	8.678		50	112	8.672	8.843	8.514
	38	86	8.629	8.686	8.708		50	114	8.599	8.715	8.523
	38	87	8.583	8.603	8.705		50	115	8.565	8.652	8.514
	38	88	8.538	8.52	8.733		50	116	8.531	8.588	8.523
Y	39	89	8.596	8.636	8.714		50	117	8.499	8.524	8.510
Zr	40	90	8.653	8.745	8.710	Sn	50	118	8.467	8.460	8.517
	40	91	8.608	8.666	8.693		50	119	8.437	8.396	8.499
	40	92	8.565	8.587	8.693		50	120	8.407	8.333	8.504
	40	94	8.483	8.429	8.667		50	122	8.351	8.205	8.488
	40	96	8.407	8.271	8.635		50	124	8.297	8.076	8.467
Nb	41	93	8.620	8.695	8.664	Sb	51	121	8.448	8.425	8.482
Mo	42	92	8.769	8.949	8.656		51	123	8.390	8.300	8.472

	42	94	8.676	8.798	8.662	Te	52	120	8.552	8.637	8.477
	42	95	8.632	8.723	8.649		52	122	8.489	8.514	8.478
	42	96	8.589	8.648	8.654		52	123	8.459	8.453	8.466
	42	97	8.548	8.572	8.635		52	124	8.430	8.391	8.473
	42	98	8.509	8.497	8.635		52	125	8.402	8.330	8.458
	42	100	8.435	8.346	8.605		52	126	8.374	8.268	8.463
Tc	43	98	8.601	8.676	8.610		52	128	8.322	8.145	8.449
	44	96	8.787	8.991	8.609		52	130	8.272	8.022	8.430
	44	98	8.696	8.847	8.620	I	53	127	8.413	8.359	8.445
	44	99	8.653	8.775	8.609		54	124	8.571	8.683	8.438
Ru	44	100	8.612	8.703	8.619		54	126	8.509	8.564	8.444
	44	101	8.572	8.631	8.601		54	128	8.451	8.446	8.443
	44	102	8.534	8.559	8.607		54	129	8.423	8.386	8.431
	44	104	8.462	8.414	8.587	Xe	54	130	8.396	8.327	8.438
Rh	45	103	8.584	8.658	8.584		54	131	8.370	8.268	8.424
	46	102	8.715	8.891	8.580		54	132	8.345	8.208	8.428
	46	104	8.633	8.754	8.586		54	134	8.296	8.089	8.414
	46	105	8.595	8.685	8.571		54	136	8.249	7.971	8.396
Pd	46	106	8.557	8.615	8.580	Cs	55	133	8.381	8.297	8.410
	46	108	8.486	8.477	8.567						
	46	110	8.420	8.339	8.547						
Ag	47	107	8.605	8.710	8.554						
	47	109	8.532	8.574	8.548						

Table 1. Continued

Nucleus	**Z**	**A**	**B/A (MINM, MeV)**	**B/A (INM. MeV)**	**B/A (EXP, MeV)**	**Nucleus**	**Z**	**A**	**B/A (MINM, MeV)**	**B/A (INM. MeV)**	**B/A (EXP, MeV)**
	56	130	8.529	8.611	8.406		68	162	8.295	8.455	8.152
Ba	56	132	8.472	8.496	8.409	Er	68	164	8.253	8.360	8.149
	56	134	8.418	8.382	8.408		68	166	8.214	8.265	8.142
	56	135	8.392	8.325	8.398		68	167	8.195	8.218	8.132

	56	136	8.366	8.267	8.403		68	168	8.176	8.170	8.130
	56	137	8.342	8.210	8.392		68	170	8.140	8.075	8.112
	56	138	8.318	8.153	8.393	Tm	69	169	8.203	8.242	8.114
La	57	138	8.377	8.295	8.375		70	168	8.132	8.403	8.112
	57	139	8.353	8.239	8.378		70	170	8.095	8.311	8.107
Ce	58	136	8.491	8.544	8.374		70	171	8.077	8.265	8.098
	58	138	8.438	8.433	8.377	Yb	70	172	8.059	8.219	8.097
	58	140	8.387	8.322	8.376		70	173	8.042	8.173	8.087
	58	142	8.339	8.212	8.347		70	174	8.025	8.126	8.084
Pr	59	141	8.422	8.403	8.354		70	176	7.992	8.034	8.064
Nd	60	142	8.317	8.481	8.346	Lu	71	175	8.050	8.196	8.069
	60	143	8.293	8.427	8.330		71	176	8.033	8.151	8.059
	60	144	8.270	8.374	8.327		72	174	8.110	8.354	8.069
	60	145	8.247	8.320	8.309		72	176	8.075	8.265	8.061
	60	146	8.224	8.267	8.304	Hf	72	177	8.057	8.220	8.052
	60	148	8.181	8.159	8.277		72	178	8.041	8.175	8.049
	60	150	8.140	8.052	8.250		72	179	8.024	8.130	8.039
Pm	61	145	8.302	8.451	8.303		72	180	8.008	8.085	8.035
Sm	62	144	8.385	8.629	8.304	Ta	73	180	8.048	8.198	8.026
	62	147	8.311	8.474	8.281		73	181	8.032	8.154	8.023
	62	148	8.288	8.422	8.280		74	180	8.090	8.308	8.025
	62	149	8.265	8.370	8.264		74	182	8.056	8.221	8.018
	62	150	8.243	8.318	8.262	W	74	183	8.040	8.177	8.008
	62	152	8.200	8.214	8.244		74	184	8.024	8.133	8.005
	62	154	8.160	8.110	8.227		74	186	7.993	8.046	7.989
Eu	63	151	8.274	8.394	8.239	Re	75	185	8.047	8.199	7.991
	63	153	8.231	8.292	8.229		75	187	8.016	8.113	7.978
Gd	64	152	8.305	8.467	8.233		76	184	8.104	8.349	7.989
	64	154	8.261	8.367	8.225	Os	76	186	8.071	8.264	7.983
	64	155	8.240	8.316	8.213		76	187	8.055	8.221	7.974
	64	156	8.219	8.266	8.215		76	188	8.039	8.179	7.974

	64	157	8.198	8.216	8.204		76	189	8.023	8.136	7.963
	64	158	8.178	8.165	8.202		76	190	8.008	8.094	7.962
	64	160	8.140	8.064	8.183		76	192	7.978	8.008	7.949
Tb	65	159	8.207	8.241	8.189	Ir	77	191	8.031	8.159	7.948
Dy	66	156	8.322	8.510	8.192		77	193	8.001	8.075	7.938
	66	158	8.278	8.412	8.190	Pt	78	190	8.085	8.305	7.946
	66	160	8.236	8.314	8.194		78	192	8.054	8.222	7.942
	66	161	8.216	8.266	8.173		78	194	8.023	8.139	7.936
	66	162	8.197	8.217	8.173		78	195	8.008	8.098	7.927
	66	163	8.177	8.168	8.162		78	198	7.965	7.973	7.914
	66	164	8.158	8.119	8.159	Au	79	197	8.015	8.120	7.916
Ho	67	165	8.186	8.193	8.147						

Table 1. Continued

Nucleus	Z	A	B/A (MINM, MeV)	B/A (INM. MeV)	B/A (EXP, MeV)
Hg	80	196	7.933	8.263	7.914
	80	198	7.904	8.183	7.912
	80	199	7.890	8.142	7.905
	80	200	7.876	8.102	7.906
	80	201	7.862	8.061	7.898
	80	202	7.849	8.020	7.897
	80	204	7.823	7.939	7.886
Ti	81	203	7.869	8.083	7.886
	81	205	7.843	8.003	7.878
Pb	82	204	7.890	8.145	7.880
	82	206	7.863	8.066	7.875
	82	207	7.850	8.026	7.870
	82	208	7.837	7.986	7.867
Bi	83	209	7.856	8.048	7.848
Po	84	209	7.889	8.147	7.835

At	85	210	7.909	8.206	7.812
Rn	86	222	7.792	7.848	7.694
Fr	87	223	7.681	7.908	7.684
Ra	88	226	7.676	7.894	7.662
Ac	89	227	7.693	7.952	7.651
Th	90	232	7.667	7.865	7.615
Pa	91	231	7.705	7.995	7.618
U	92	234	7.700	7.980	7.601
	92	235	7.690	7.944	7.591
	92	238	7.659	7.838	7.570
Np	93	237	7.566	7.965	7.575
Pu	94	244	7.524	7.812	7.525
Am	95	243	7.557	7.937	7.530
Cm	96	247	7.544	7.889	7.502
Bk	97	247	7.568	7.977	7.499
Cf	98	251	7.554	7.93	7.471
Es	99	252	7.439	7.982	7.457
Fm	100	257	7.418	7.903	7.422
Md	101	258	7.431	7.955	7.410
No	102	259	7.444	8.006	7.400
Lr	103	261	7.449	8.024	7.381
Rf	104	267	7.420	7.917	7.342
Db	105	268	7.304	7.966	7.328
Sg	106	269	7.316	8.015	7.318
Bh	107	274	7.297	7.941	7.278
Hs	108	275	7.309	7.989	7.267
Mt	109	276	7.320	8.036	7.250
Ds	110	281	7.302	7.964	7.219
Rg	111	282	7.183	8.011	7.204
Cn	112	285	7.180	7.998	7.184
Nh	113	286	7.191	8.044	7.168

Fr	114	289	7.188	8.031	7.148
Mc	115	290	7.198	8.076	7.130
Lv	116	293	7.195	8.063	7.111
Ts	117	294	7.074	8.107	7.092
Og	118	294	7.091	8.177	7.079

The calculations of the binding fractions obtained from the modified integrated nuclear model (MINM) as shown in Table 1, yields a root mean square deviation of 0.2667 MeV with respect to experimental binding energy data. Similarly, the root mean square deviations for the binding fraction obtained using integrated nuclear model yields 1.5801 MeV. This shows that, MINM calculations are relatively closer to the experimental data than the INM for the 318 nuclides investigated.

Comparatively, there is a very good agreement between the binding fraction values calculated using the MINM and the experimental values for the binding fraction of nuclei. The root mean square deviation is very small (0.2667 MeV) and this very much supports the validity of the MINM, and the consequent accuracy in the values of the binding fraction for different nuclei. For instance, ${}^{16}_{8}\mathrm{O}$, ${}^{22}_{10}\mathrm{O}$ ${}^{44}_{20}\mathrm{Ca}$, ${}^{51}_{23}\mathrm{V}$, ${}^{53}_{24}\mathrm{Cr}$, ${}^{58}_{26}\mathrm{Fe}$, ${}^{68}_{30}\mathrm{Zn}$, ${}^{94}_{42}\mathrm{Mo}$, ${}^{95}_{42}\mathrm{Mo}$, ${}^{98}_{43}\mathrm{Tc}$, ${}^{100}_{44}\mathrm{Ru}$, ${}^{103}_{45}\mathrm{Rh}$, ${}^{104}_{46}\mathrm{Pd}$, ${}^{106}_{46}\mathrm{Pd}$, ${}^{109}_{47}\mathrm{Ag}$, ${}^{111}_{48}\mathrm{Cd}$, ${}^{117}_{50}\mathrm{Sn}$, ${}^{128}_{54}\mathrm{Xe}$, ${}^{129}_{54}\mathrm{Xe}$, ${}^{134}_{56}\mathrm{Ba}$, ${}^{135}_{56}\mathrm{Ba}$, ${}^{138}_{57}\mathrm{La}$, ${}^{140}_{58}\mathrm{Ce}$, ${}^{142}_{58}\mathrm{Ce}$, ${}^{145}_{61}\mathrm{Pm}$, ${}^{148}_{62}\mathrm{Sm}$, ${}^{152}_{62}\mathrm{Sm}$, ${}^{156}_{64}\mathrm{Gd}$, ${}^{164}_{66}\mathrm{Dy}$, ${}^{170}_{70}\mathrm{Yb}$, ${}^{171}_{70}\mathrm{Yb}$, ${}^{176}_{72}\mathrm{Hf}$, ${}^{177}_{72}\mathrm{Hf}$, ${}^{181}_{73}\mathrm{Ta}$, ${}^{198}_{78}\mathrm{Pt}$, ${}^{196}_{80}\mathrm{Hg}$, ${}^{198}_{80}\mathrm{Hg}$, ${}^{203}_{81}\mathrm{Ti}$, ${}^{206}_{82}\mathrm{Pb}$, ${}^{209}_{83}\mathrm{Bi}$, ${}^{226}_{88}\mathrm{Ra}$, ${}^{237}_{93}\mathrm{Np}$, ${}^{244}_{94}\mathrm{Pu}$, ${}^{269}_{106}\mathrm{Sg}$, ${}^{285}_{112}\mathrm{Cn}$, ${}^{294}_{118}\mathrm{Og}$ and so on.

The graphical illustrations for the binding fractions calculated using INM, MINM and experimental data are shown in Figure 1 and Figure 2.

The scatter plot in Figure 1 shows the curve of the binding energy per nucleon against the mass numbers for the calculations obtained from INM, and the experimental data obtained from the atomic mass evaluation tables (AME2016) [37]. The red scatter plot shows the data obtained from INM while the green scatter plot shows the experimental data. It is noted that, from A>220 (the heavy and super heavy nuclei) the binding fractions for the INM data rise steadily while the experimental binding fractions decrease uniformly.

This increase in the values of the binding fraction for the INM data may be attributed to the effects resulting from the deformed shapes of the heavy and super heavy nuclei. It was found that, this behavior can be corrected by the introduction of the quantity $\sqrt{NZ}$ as the divisor and the variable stability coefficient λ, in the second term of the MINM as written in Eq. (3). The graphical illustration is shown in Figure 2.

In Figure 2, the red scatter plot shows the data obtained from MINM while the green scatter plot shows the experimental data. The rise in the binding fractions that was noted in Figure 1 for Z>220 has been corrected by the introduction of the divisor $\sqrt{NZ}$ and the variable stability coefficient λ. Despite the fact that the MINM does not generate the exact values of the binding fractions as obtained from the experimental data, the MINM takes us relatively closer to the experimental binding energies. Thus, contributing towards the attainment of the primary objectives of theoretical nuclear physics.

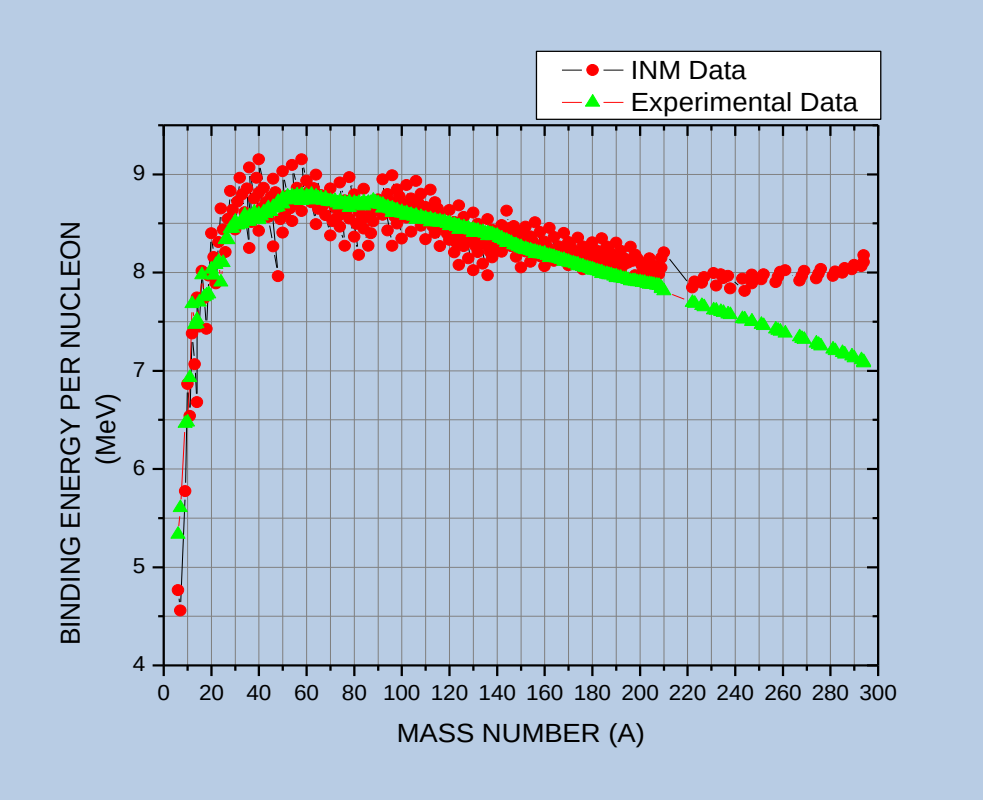

Figure 1. The integrated nuclear model data in comparison with the experimental data of nuclear binding fraction.

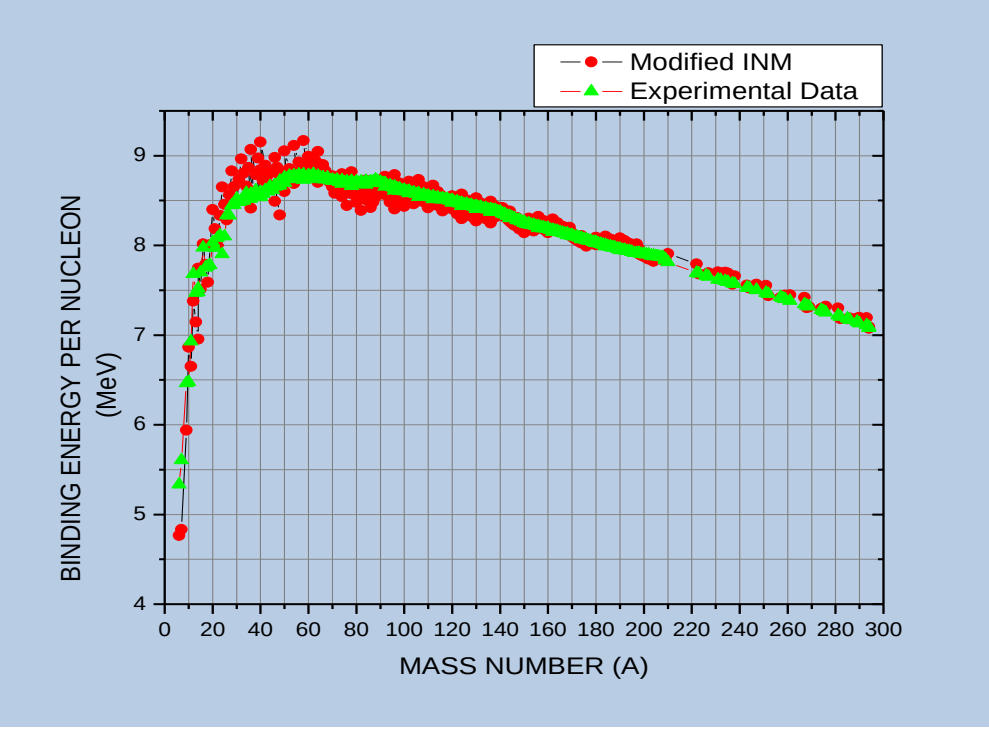

Figure 2: The Modified integrated nuclear model data in comparison with the experimental data of nuclear binding fraction.

5. CONCLUSIONS

The modified binding energy equation based on the INM has been formulated. The formula is relatively simple since it depends only on the proton and neutron numbers and a single variable parameter denoted by λ. In addition, the model allows better prediction of the binding energies more than other theoretical models such as the LDM and INM, especially in the region where A>220. This is attributed to the fact that, it was developed based on the theory of quantum chromodynamics. In order to check the validity of the MINM, the values of root mean square deviations were computed. It was found that, the root mean square deviation for the binding fractions obtained from the MINM is 0.2667 MeV with respect to experimental binding energy data. Similarly, the root mean square deviation for the binding fractions obtained from the integrated nuclear model is 1.

5801 MeV. This implies that, MINM provides a very good degree of accuracy, and this supports the validity of the MINM and the consequent accuracy in the values of the binding fraction for different nuclei. Therefore, the MINM can be applied in determining the binding energies of designer nuclei based on the fact that, there is inadequate experimental information on such kind of nuclei. Nonetheless, the MINM is still open to further improvement especially in the region whereby A<5.

References

[1] Reid, J. M. (1984). The atomic nucleus. Manchester University Press.

[2] Ghoshal, S. N. (2008). Nuclear physics. S. Chand Publishing.

[3] Davies, P. C. W., & Brown, J. R. (1993). *The ghost in the atom: a discussion of the mysteries of quantum physics*. Cambridge University Press.

[4] Michimasa, S., Kobayashi, M., Kiyokawa, Y., Ota, S., Ahn, D. S., Baba, H., & Ideguchi, E. (2018). Magic Nature of Neutrons in Ca 54: First Mass Measurements of Ca 55–57. *Physical Review Letters*, 121(2), 022506

[5] Adamian, G. G., Antonenko, N. V., Diaz-Torres, A., & Heinz, S. (2020). How to extend the chart of nuclides? *The European Physical Journal A*, 56(2), 1-51

[6] National Research Council. (1986). Nuclear physics. National Academy Press.

[7] Rabinowitz, M. (2015). General derivation of mass-energy relation without electrodynamics or Einstein's postulates. *Journal of Modern Physics*, 6(09), 1243

[8] Chemogos, P. K., Muguro, K. M., & Khanna, K. M. (2019). Modified Phenomenological Formula for the Ground State Energy of Light Nuclei. *World Scientific News*, 136, 148-158

[9] Oganessian, Y. (2012). Nuclei in the Island of Stability of Superheavy Elements. *Journal of Physics-Conference Series* Vol. 337, No. 1, p. 012005

[10] Williams, M. (2016). What is binding energy? Universe Today: Space and Astronomy News

[11] Oganessian, Y. T., & Utyonkov, V. K. (2015). Super-heavy element research. *Reports on Progress in Physics*, 78(3), 036301

[12] Weizsäcker, C. F. V. (1935). On the theory of nuclear masses. *Journal of Physics*, 96, 431-458

[13] Mishra, A., Gupta, T., & Sahu, B. (2016). Estimation of Nuclear Separation Energy and Its Relation with Q Value. *International Journal of Applied Physics and Mathematics*, 6(1), 17

[14] Bohr, N., & Wheeler, J. A. (1939). The mechanism of nuclear fission. *Physical Review*, 56(5), 426.

[15] Bethe, H. A., & Bacher, R. F. (1936). Nuclear physics A. Stationary states of nuclei. *Reviews of Modern Physics*, 8(2), 82

[16] Dai, H., Wang, R., Huang, Y., & Chen, X. (2017). A novel nuclear dependence of nucleon–nucleon short-range correlations. *Physics Letters B*, 769, 446-450

[17] Heyde, K. (2004). Basic ideas and concepts in nuclear physics: an introductory approach. CRC Press.

[18] Royer, G. (2000). Alpha emission and spontaneous fission through quasi-molecular shapes. *Journal of Physics G: Nuclear and Particle Physics*, 26(8), 1149

[19] Kirson, M. W. (2008). Mutual influence of terms in a semi-empirical mass formula. *Nuclear Physics A*, 798(1-2), 29-60

[20] Ghahramany, N., Gharaati, S., & Ghanaatian, M. (2012). New approach to nuclear binding energy in integrated nuclear model. *Journal of Theoretical and Applied Physics*, 6(1), 3.

[21] Bailey, D. (2011). Semi-empirical nuclear mass formula. PHY357: Strings & Binding Energy. University of Toronto, 03-31

[22] Samanta, C., Chowdhury, P. R., & Basu, D. N. (2006). Generalized mass formula for non-strange and hypernuclei with SU (6) symmetry breaking. *Journal of Physics G: Nuclear and Particle Physics*, 32(3), 363

[23] Chowdhury, P. R., Samanta, C., & Basu, D. N. (2005). Modified Bethe–Weizsäcker Mass Formula with Isotonic Shift and new Driplines. *Modern Physics Letters A*, 20(21), 1605-1618

[24] Sirma, K. K., Chelimo, L. S., & Khanna, K. M. (2020). A modified Nuclear Model for Binding Energy of Nuclei. *World Scientific News*, 143, 203-223

[25] Seshavatharam, U. V. S., & Lakshminarayana, S. (2017). Simplified Form of the Semi-empirical Mass Formula. *Prespacetime Journal*, Volume 8, Issue 4, pp. 881-890

[26] Mahdi Joharifard and Mohammad Reza Pahlavani. (2018). Binding Energies of Deformed Super Heavy Nuclei with $Z \geq 105$. *BAOJ Physics*, 3, 28

[27] Van Isacker, P. (2007). Global and local nuclear mass formulas. In *XXX Mazurian Lakes Conference Nuclear Physics and The Fundamental Processes*, Vol. 39, pp. 421-431

[28] Kolesnikov, N. N. (2016). The binding energies and stability of heavy and superheavy nuclei. *Moscow University Physics Bulletin*, 71(4), 381-388

[29] Hwang, M. Y. The E-space Inter-Domain Interaction Potential (EIDIP) Model. Retrieved from: https://www.researchgate.net/publication/235782325

[30] Hwang, M. Y. (2013). EIDIP nuclear charge radii model. Retrieved from: https://www.researchgate.net/profile/Michael_Hwang/publication/235782273

[31] Audi, G., Wapstra, A. H., & Thibault, C. (2003). The AME2003 atomic mass evaluation: (II). Tables, graphs and references. *Nuclear Physics A*, *729*(1), 337-676

[32] Ghahramany, N., Hora, H., Miley, G. H., Philberth, K., & Osman, F. (2008). Nuclear magic numbers based on a quark-like model is compared with the Boltzmann distribution model from nuclear abundance in the universe and low energy nuclear reactions. *Physics Essays*, 21(3), 200-206

[33] Ghahramany, N., Ghanaatian, M., & Hooshmand, M. (2007). Quark-gluon plasma model and origin of magic numbers. *Iranian Physical Journal*, 1-2, 35

[34] Ghahramany, N., Gharaati, S., Ghanaatian, M., & Hora, H. (2011). New scheme of nuclide and nuclear binding energy from quark-like model. *Iranian Journal of Science and Technology (Sciences)*, 35(3), 201-208

[35] Ghahramany, N., Sarafraza, H., & Yazdankish, E. (2013). Stability and mass parabola in integrated nuclear model. *Universal Journal of Physics and Application*, 1(1), 18-25.

[36] Seshavatharam, U. V. S., & Lakshminarayana, S. A (2020). A new kind of unified nuclear binding energy formula and its consequences. Retrieved from: https://doi.org/10.35543/osf.io/qyge6

[37] Wang, M., Audi, G., Kondev, F. G., Huang, W. J., Naimi, S., & Xu, X. (2017). The AME2016 atomic mass evaluation (II). Tables, graphs and references. *Chinese Physics C*, 41(3), 030003